Free Radical Biology and Medicine 75 (2014) 48–59

Contents lists available at ScienceDirect

Free Radical Biology and Medicine

journal homepage: www.elsevier.com/locate/freeradbiomed

Original Contribution

Oxidized LDL lipids increase β-amyloid production by SH-SY5Y cells through glutathione depletion and lipid raft formation

Irundika H.K. Dias [a], Jayna Mistry [a], Shaun Fell [a], Ana Reis [a], Corinne M. Spickett [a], Maria C. Polidori [b], Gregory Y.H. Lip [c], Helen R. Griffiths [a,*]

[a] Life and Health Sciences and Aston Research Centre for Healthy Ageing, Aston University, Birmingham, West Midlands B4 7ET, UK
[b] Institute of Geriatrics, University of Cologne, Cologne, Germany
[c] Centre for Cardiovascular Sciences, City Hospital Birmingham, Birmingham B18 7QH, UK

ARTICLE INFO

Article history:
Received 31 March 2014
Received in revised form
17 June 2014
Accepted 9 July 2014
Available online 15 July 2014

Keywords:
OxLDL
GSH
Redox
Aging
BACE1
Lipid raft
Low-density lipoprotein
Cholesterol
Lipid oxidation
Free radicals

ABSTRACT

Elevated total cholesterol in midlife has been associated with increased risk of dementia in later life. We have previously shown that low-density lipoprotein (LDL) is more oxidized in the plasma of dementia patients, although total cholesterol levels are not different from those of age-matched controls. β-Amyloid (Aβ) peptide, which accumulates in Alzheimer disease (AD), arises from the initial cleavage of amyloid precursor protein by β-secretase-1 (BACE1). BACE1 activity is regulated by membrane lipids and raft formation. Given the evidence for altered lipid metabolism in AD, we have investigated a mechanism for enhanced Aβ production by SH-SY5Y neuronal-like cells exposed to oxidized LDL (oxLDL). The viability of SH-SY5Y cells exposed to 4 μg oxLDL and 25 μM 27-hydroxycholesterol (27OH-C) was decreased significantly. Lipids, but not proteins, extracted from oxLDL were more cytotoxic than oxLDL. In parallel, the ratio of reduced glutathione (GSH) to oxidized glutathione was decreased at sublethal concentrations of lipids extracted from native and oxLDL. GSH loss was associated with an increase in acid sphingomyelinase (ASMase) activity and lipid raft formation, which could be inhibited by the ASMase inhibitor desipramine. 27OH-C and total lipids from LDL and oxLDL independently increased Aβ production by SH-SY5Y cells, and Aβ accumulation could be inhibited by desipramine and by *N*-acetylcysteine. These data suggest a mechanism whereby oxLDL lipids and 27OH-C can drive Aβ production by GSH depletion, ASMase-driven membrane remodeling, and BACE1 activation in neuronal cells.

Alzheimer's disease (AD)[1] is the most common neurodegenerative disease and is characterized by progressive decline in cognitive performance with loss of memory, orientation, and judgment [1]. Loss of synapses and cholinergic neurons, accumulation of extracellular Aβ plaques, and intraneuronal neurofibrillary tangles of hyperphosphorylated tau are major hallmarks of the AD brain [1].

Aβ is derived from amyloid precursor protein (APP), an abundant type I membrane protein that is a substrate for at least three proteolytic ("secretase") activities designated α, β, and γ. The major proteolytic pathway, undergone by ~95% of the APP in neurons, is α–γ, i.e., APP is first cleaved by an α-secretase within the Aβ region and subsequently by the γ-secretase. The second proteolytic pathway, which leads to the formation of Aβ, is the β–γ pathway. In this case, APP is first cleaved by the β-secretase β-site amyloid cleaving enzyme (BACE1), a membrane-spanning aspartic protease, with further processing by the γ-secretase to produce the 4-kDa Aβ peptide [2]; the initial cleavage of APP by BACE1 is the rate-limiting step for Aβ production in AD brains.

Lipids are key regulators of brain function and have been increasingly implicated in neurodegenerative disorders, including AD; a major risk factor for late-onset AD is the ε4 allelic variant of ApoE, which encodes a protein involved in cholesterol metabolism and lipid transport [3]. Importantly, a variety of genes have been

Abbreviations: AD, Alzheimer disease; Aβ, β-amyloid; APP, amyloid precursor protein; ASMase, acid sphingomyelinase; BACE, β-secretase β-site amyloid cleaving enzyme; BBB, blood–brain barrier; BCA, bicinchoninic acid; BHT, butylated hydroxytoluene; BSO, buthionine sulfoximine; CSF, cerebrospinal fluid; CTB, cholera toxin B; E-64, proteinase inhibitor E-64; EDTA, ethylenediamine tetraacetic acid; EGTA, ethylene glycol tetraacetic acid; ESI–MS, electrospray ionization mass spectrometry; ELISA, enzyme-linked immunosorbent assay; GCL, glutamate–cysteinyl ligase; GSSG, oxidized glutathione; GSH, glutathione; LDL, low-density lipoprotein; MDA, malondialdehyde; NAC, *N*-acetylcysteine; 27OH-C, 27-hydroxycholesterol; oxLDL, oxidized low-density lipoprotein; PBS, phosphate-buffered saline; PBST, phosphate-buffered saline with 1% Tween 20; PVDF, polyvinylidene fluoride; SM, sphingomyelin; SDS–PAGE, sodium dodecyl sulfate–polyacrylamide gel electrophoresis

* Corresponding author. Fax: +44 0 121 359 0357.
E-mail address: helen.griffiths@aston.ac.uk (H.R. Griffiths).

http://dx.doi.org/10.1016/j.freeradbiomed.2014.07.012

recently linked to late-onset AD through genome-wide association studies and are directly or indirectly connected to lipid metabolism or cellular membrane dynamics [4,5].

In support of a role for lipids in AD, Chan et al. [6] analyzed the prefrontal cortex, entorhinal cortex, and cerebellum of late-onset AD patients and found an elevation of diacylglycerol and sphingolipids in the prefrontal cortex of AD patients. Enrichment of lysobisphosphatidic acid, sphingomyelin, the ganglioside GM3, and cholesterol esters was observed in the affected entorhinal cortex but no change in lipids occurred within the cerebellum. Most recently, a fingerprint of 10 plasma lipids that defines AD presence has been identified in older adults [7]; however, it is unknown whether they play a mechanistic role in disease development or progression.

Membrane lipids are involved in the trafficking and/or activity of the key membrane-bound proteins controlling Aβ levels, including APP, BACE1, and presenilins; first, the regulation of BACE1 activity is determined by its access to APP, which is in turn lipid-dependent and involves lipid raft formation; three groups of lipids that stimulate proteolytic activity of BACE are (1) neutral glycosphingolipids (cerebrosides), (2) anionic glycerophospholipids, and (3) cholesterol [8]; second, γ-secretase activity is regulated by membrane levels of cholesterol and sphingomyelin (SM) [9]. The enzymes most strongly implicated in regulation of these lipids are HMG-CoA reductase and sphingomyelinase. Third, lipids such as ganglioside GM1 modulate the pathogenic potential of Aβ by affecting its propensity to aggregate [10]. Cholesterol is highly enriched in the brain and is a major constituent of normal neuronal membranes. Whereas brain cholesterol homeostasis is regulated through de novo synthesis and is normally segregated from peripheral circulation owing to the impermeability of the blood–brain barrier (BBB) [11,12], oxysterols such as 27-hydroxycholesterol (27OH-C) are known to cross the blood–brain barrier more readily than cholesterol [13,14]. Moreover, 27OH-C has been shown to accumulate in AD brains [15] and aberrant lipid homeostasis is implicated in AD [16]. In contrast, the related 24OH-C is produced within the brain and is found at raised levels in plasma from AD patients

Not only cholesterol is transported by lipoproteins; for example, SMs are transported by low-density lipoproteins (LDL) [17] and high-density lipoproteins carry carotenoids and ApoA1, and lower concentrations of either are independent risk factors for AD [18,19]. We have previously shown in a population of older adults that oxidized LDL is increased in AD patients with vascular risk factors compared to age-matched control subjects [11]. Levels of protein carbonyls on LDL were associated with cognitive impairment, although total cholesterol levels were not different from those of age-matched controls [11].

Exposure of a variety of cells to oxLDL can trigger intracellular oxidative stress and glutathione (GSH) depletion [20]. GSH is consumed in the detoxification of lipid peroxidation products, catalyzed by GSH peroxidase. According to the extent of lipid peroxide burden, GSH loss is usually transient and after several hours is restored through de novo synthesis. Lipid raft formation is also accelerated during oxidative stress, as the activity of sphingomyelinase, an enzyme responsible for cleaving membrane sphingolipids, is increased by GSH depletion [21]. This illustrates a relationship between extracellular lipoprotein oxidation, intracellular redox imbalance, and membrane remodeling, although the nature of the molecules in oxLDL that mediate this effect is unknown.

Others have shown recently that 27OH-C increases BACE1 levels in hippocampal organotypic slices from adult rabbits [22] and in human SH-SY5Y neuroblastoma cells [23]. These studies have also demonstrated that Gadd153 and nuclear factor-κB regulate BACE1 expression in a concerted fashion in response to 27OH-C [24]. These studies provide evidence that BACE1 expression is important for Aβ formation; however, they do not examine the effect of 27OH-C on the pathway, e.g., in membrane reorganization that is required for BACE1 activation, nor has the (patho) physiological source of 27OH-C been investigated.

Recognizing the association of systemic hypercholesterolemia in midlife with AD in later life, we have therefore investigated the hypothesis that systemically oxidized 27OH-C and oxidized lipids in general derived from oxLDL in plasma deplete GSH in neuronal cells, promote lipid raft formation through enhanced sphingomyelinase activity, and increase Aβ formation. Our approach to identifying novel pathways for reducing toxic Aβ formation through improved understanding of 27OH-C effects and production upstream of Aβ is an important strategy in the search for new therapeutic targets.

Materials and methods

Cell culture

The neuroblastoma cell line SH-SY5Y from the American Type Culture Collection was maintained in RPMI 1640 medium (Gibco) containing 10% fetal bovine serum, 1% nonessential amino acids, and 200 U/ml penicillin and streptomycin at 37 °C in a humidified atmosphere of 5% CO_2 and 95% air. All reagents were from Sigma unless otherwise stated.

Isolation, modification, and characterization of LDL

Blood for lipoprotein isolation was drawn from the antecubital vein of normolipemic healthy volunteers into EDTA after 12 h of fasting. Control subject LDL for in vitro oxidation and analysis was from healthy controls recruited at Aston University who showed no evidence of cognitive impairment. Ethical approval was obtained from the Aston University ethics committee. None of the volunteers were taking antioxidant supplements.

AD subjects were recruited from the Unit of Cognitive Frailty, Neurology Outpatient Clinic, Cologne, Germany, after diagnosis of AD using NINCDS–ADRDA criteria [7]. Informed consent was obtained from the patients or their caregivers according to severity of disease by the local ethics committee.

LDL was isolated from plasma by density-gradient ultracentrifugation with potassium bromide (KBr) as previously described [25,26]. To remove residual KBr and EDTA before starting the in vitro oxidation reaction, the LDL was passed through a PD-10 column (GE Healthcare, Little Chalfont, UK). OxLDL was prepared by incubating with 10 μM $CuSO_4$ for 1 h at 37 °C and then the reaction was stopped by adding 10 °μM EDTA as previously described [26]. Copper and EDTA were then removed by passing the samples through PD-10 columns (GE Healthcare) against phosphate-buffered saline (PBS). To sterilize and remove aggregates, both LDL and oxLDL were filtered through a 0.22-μm filter (Millipore), stored under nitrogen in the dark at 4 °C, and used within 2 weeks of preparation. To ensure the LDL did not undergo further oxidation, the MDA concentration was measured as thiobarbituric acid-reactive substances. MDA concentration was not affected significantly (2.5 ± 0.1 versus 2.6 ± 0.08 nmol MDA/mg for LDL and 3.8 versus 3.9 ± 0.6 nmol MDA/mg for oxLDL) after storage. The final protein concentration was determined by bicinchoninic acid assay (BCA assay) against a bovine serum albumin standard and the amounts of LDL used in experiments are described by protein content. The purity and charge of LDL and oxLDL were evaluated by examination of electrophoretic migration in a 1% agarose gel. 8-Isoprostane F2α levels in LDL and oxLDL were measured by ELISA (Cayman Chemicals, Ann Arbor, MI, USA).

Extraction of lipids and proteins from LDL

LDL lipids (LDL-L) were extracted from LDL using the Folch method by addition of 160 μl of ice-cold methanol (containing 50 μg/ml BHT) followed by the addition of 320 μl of ice-cold chloroform and incubation for 20 min on ice with occasional vortex mixing. High-purity water (150 μl) was added and the sample kept on ice for an additional 10 min with occasional mixing. The sample was centrifuged for 5 min at 2000*g* and the upper (aqueous) phase was removed and reextracted by addition of 250 μl of ice-cold chloroform:methanol (2:1, v/v) as above. The upper phase was discarded and both organic phases were combined, dried under nitrogen gas, and kept at −80 °C until further use. Extracted lipids for cell culture experiments were conjugated to fatty acid-free bovine serum albumin (BSA) in serum-free RPMI 1640 [25].

Cell culture treatments

SH-SY5Y cells (5×10^5/ml) were incubated overnight at 37 °C in a humidified atmosphere. Cells received RPMI medium replacement before 2 h of each treatment. Cells were treated with 0.8–8 μg/ml LDL-L or oxLDL-L or 2.5–25 μM 27OH-C for 2 or 16 h. SH-SY5Y cells were cotreated with 10 μM desipramine or 3 mM *N*-acetylcysteine (NAC) for 2 or 16 h. To measure secretory forms of Aβ, the medium was removed from SH-SY5Y cells and replaced with 2 ml of reduced-serum medium (Opti-MEM). Cells were treated with 4 μg/ml LDL, 4 μg/ml oxLDL, or an equal volume of medium for 16 h. Supernatants were transferred into a microcentrifuge tube and centrifuged to remove any dead cells, then the clear supernatant was transferred into a new microcentrifuge tube and vacuum concentrated down to 100 μl.

3-(4,5-Dimethylthiazol-2-yl)-2,5-diphenyltetrazolium (MTT) assay

Four hours before the completion of each experiment, SH-SY5Y cells were incubated with MTT solution (1 mg/ml) at 37 °C and analyzed for metabolic activity compared to untreated controls [18].

Measurement of intracellular GSH and oxidized glutathione (GSSG)

After 2 or 16 h of incubation, 27OH-C, LDL, oxLDL, extracted-lipid-treated, and untreated control SH-SY5Y (5×10^5) cells were centrifuged and washed twice with PBS. Sulfosalicylic acid (3.33 μl of 100% in distilled water) was then added to the cell pellet and GSH and GSSG levels were assessed by the GSH recycling assay as described by Qin et al. [27]. Protein concentration was measured using the BCA assay.

Acid sphingomyelinase (ASMase) activity assay

ASMase activity in SH-SY5Y cells was measured as described previously with some modifications [21]. Control and treated SH-SY5Y cells (1×10^7) were centrifuged and washed with ice-cold PBS to remove the medium. The cell pellet was resuspended in 1 ml of lysis buffer (25 mM Tris–HCl buffer (pH 5), 2 mM EDTA, 2 mM EGTA, 1 mM phenylmethylsulfonyl fluoride, 20 μg/ml E-64). Cell extracts were homogenized by passing five times through a 25-gauge needle and used as the enzyme source.

The assay buffer (200 μl) consisted of 15 mM 2-*N*-hexadecanoylamino-4-nitrophenylphosphorylcholine (Calbiochem, San Diego, CA, USA), 100 mM Tris–HCl buffer (pH 5), 10 mM $MgCl_2$, and 10 μl of the cell extract. Incubation followed at 37 °C for 60 min; the enzyme reaction was terminated by adding 400 μl of 100 mM glycine buffer (pH 10.5) and 700 μl of ethanol. The suspension was vortexed and centrifuged at 2000*g* for 10 min. The absorbance of the supernatant solution was measured spectrophotometrically at 410 nm.

Isolation of lipid raft microdomains by gradient centrifugation

Lipid rafts were isolated as previously described [28]. SH-SY5Y cells (1×10^7 cells) were lysed in 1 ml of MNE buffer (150 mM NaCl, 2 mM EDTA, 25 mM 2-(N-morpholino)ethanesulfonic acid, with 1% protease inhibitor cocktail, pH 6.5) containing 1% Triton X-100 on ice for 30 min. Cell extracts were homogenized by five passages through a 21-gauge needle. Lysates were obtained by centrifuging at 14,000*g*, 4 °C, for 5 min to remove the nuclei and insoluble materials. The cell lysates (1 ml) were mixed 1:1 with 85% sucrose solution, layered in the bottom of the centrifuge tube (Ultra Clear Beckman centrifuge tubes), and overlaid sequentially with 6 ml of 30% and 3.5 ml of 5% sucrose solution to make a noncontinuous sucrose gradient. Samples were centrifuged at 20,000*g* for 16 h at 4 °C using an SW41Ti rotor (Beckman). Fractions (1 ml) numbered 1–9 were collected from the top of the tube downward and proteins in each fraction were precipitated with 5% trichloroacetic acid for 30 min on ice.

Proteins in lipid raft fractions were isolated by centrifugation at 13,000*g*, 4 °C, for 15 min. The protein pellet was carefully washed with cold acetone twice, air dried, and then resuspended in modified Laemmli buffer (4 M urea, 0.2% ABF-14, 20% dimethyl sulfoxide, 4% SDS, 20% glycerol, 10% 2-mercaptoethanol, 0.004% bromophenol blue, and 0.125M Tris–HCl, pH 6.8). Samples were heated 5 min at 95 °C before storage at −20 °C for later analysis by Western blot.

Western blot for analysis of lipid rafts

For immunodetection of lipid-raft-associated proteins, 15 μl of each fraction in modified Laemmli buffer was subjected to 10% SDS–PAGE, transferred onto a PVDF membrane, and blocked with 3% BSA. The membrane was probed with the primary monoclonal antibody anti-flotillin-1 (1:1000, BD Biosciences) for 2 h at room temperature followed by extensive washing and then incubation with horseradish peroxidase-labeled anti-rabbit IgG (1:5000) for 2 h. The immunoreactive bands were detected by enhanced chemiluminescence methods (GE Healthcare).

Confocal imaging

To stain lipid rafts, SH-SY5Y cells were rinsed with chilled growth medium and then incubated with 1 μg/ml cholera toxin B (CTB)–Alexa Fluor 488 at 4 °C for 15 min before fixation in 4% paraformaldehyde. CTB binds to lipid rafts with some limited specificity toward ganglioside GM1 [29]. Coverslips were mounted in Anti-Fade DAPI-Fluoromount-G (SouthernBiotech, Birmingham, AL, USA) and viewed using a Leica confocal microscope (Leica Microsystems, Wetzlar, Germany).

β-Amyloid ELISA

A sandwich ELISA was performed to detect secreted β-amyloid levels. The ELISA plate was incubated at 4 °C overnight with β-amyloid, 1-16 (6E10) monoclonal antibody (Covance Research Products, Denver, PA, USA), followed by washing with PBST. BSA (3%) in PBS was used to block for 1 h and then washed with PBST. A standard curve from 0 to 2.5 nmol/L of β-amyloid protein standard was prepared. Samples of LDL, oxLDL, and their respective lipid- and control-treated culture media were adjusted to 20 μg/ml protein in carbonate buffer and incubated for 2 h. Anti-β-amyloid antibody was added and incubated for 1 h, followed by washing with PBST and incubation with anti-rabbit peroxidase

conjugate antibody for 30 min. After a thorough washing with PBST, citrate buffer (with hydrogen peroxide and *o*-phenylenediamine) was added with detection at 490 nm.

Electrospray ionization mass spectrometry (ESI–MS)

Oxidized cholesteryl esters were identified by scanning for precursors of *m/z* 369. Extracted lipid samples were initially dissolved in a small volume of chloroform:methanol (1:1, v/v) and then diluted 10 times into 200 μl of 0.1 mM ammonium acetate in methanol. Samples were analyzed by ESI in positive-ion mode on a QTrap5500 instrument (ABSciex, Warrington, UK) by direct infusion at a flow rate of 5 μl/min. The spray capillary voltage was set at 5500 V and declustering potential at 50 V, with a curtain gas setting of 20 and a source temperature of 150 °C. For the precursor ion scans the precursor of *m/z* 369.0 Da was selected with unit resolution in both quadrupoles, a collision energy of 30 V, and an *m/z* range of 200–1000 at 5 s/scan with a 0.1-Da step size. For each spectrum 100–500 scans were averaged. Further confirmation of the occurrence of lipid oxidation in oxLDL compared to the control LDL was undertaken by analysis of phospholipids in the positive-ion ESI mode. Phosphatidylcholines (PCs) were identified by scanning for precursors of the phosphocholine fragment ion at *m/z* 184 as described above for cholesterol with the following changes: precursor of *m/z* 184.1, collision energy 47 V, declustering potential 65 V, mass range *m/z* 300–1000 Da, and scan time 7 s. Oxidized PCs were identified from their monoisotopic mass.

Data analysis

Data were analyzed using GraphPad Prism software (version 5). Unless specified all data are presented as the mean ± SEM of at least three independent experiments, each performed in triplicate. Statistical analysis was performed using analysis of variance followed by Tukey's multiple comparison test.

Results

27OH-C decreases SH-SY5Y GSH/GSSG ratio and increases Aβ secretion

To understand the effects of oxidized molecules on neuronal cells, we sought to establish concentrations of 27OH-C that

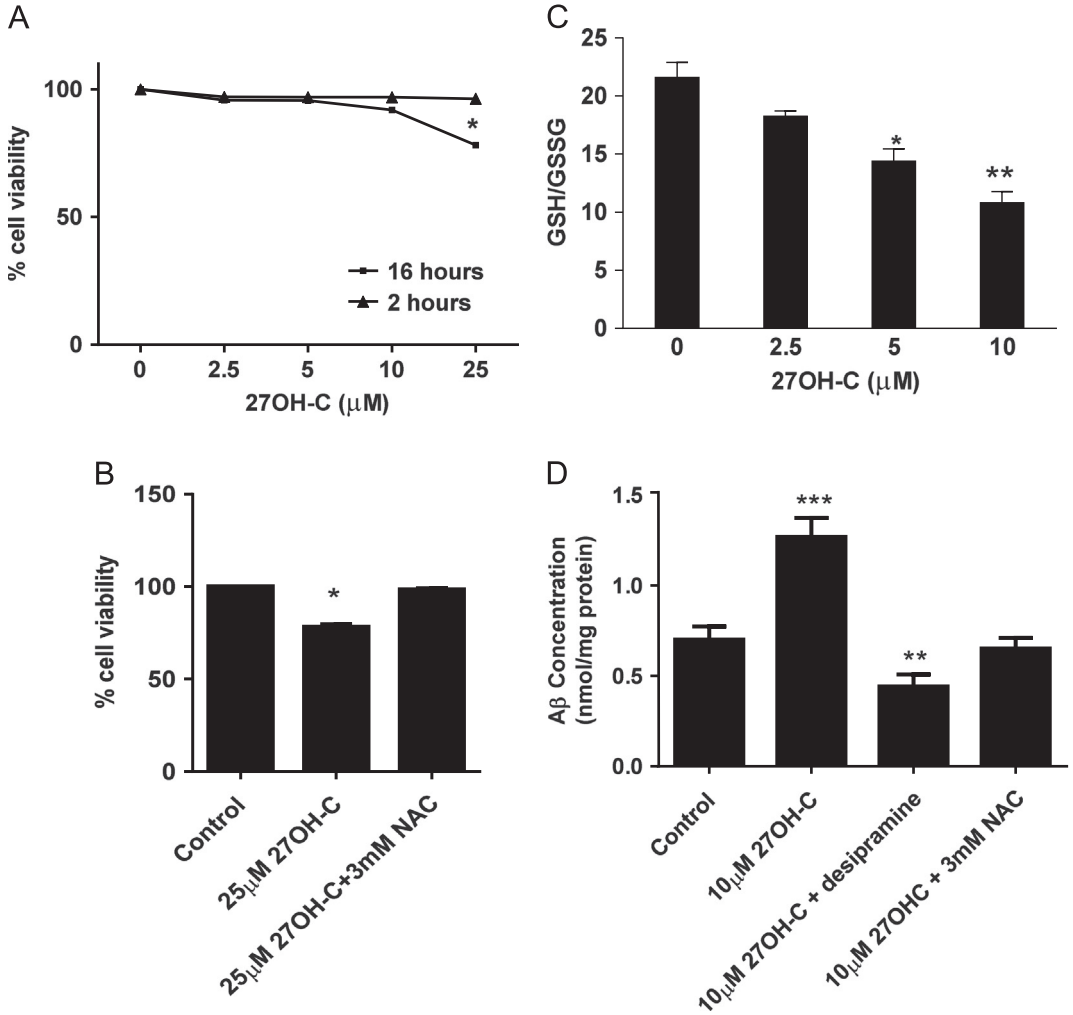

Fig. 1. Effects of 27OH-C on SH-SY5Y cell viability, GSH level, and Aβ secretion. (A) SH-SY5Y cells were challenged with 2.5–25 μM 27OH-C for 16 h and cell viability was measured by MTT assay. (B) SH-SY5Y cells (2×10^4) were challenged with 10 μM 27OH-C for 16 h in the presence or absence of 3 mM NAC. (C) Intracellular GSH and GSSG levels were measured, after treating cells with 2.5–10 μM 27OH-C for 2 h, by the GSH recycling assay and the GSH/GSSG ratio is shown. (D) Protein levels were measured by BCA assay. Results are from three independent experiments. Significant differences were calculated using one-way ANOVA followed by Tukey's multiple comparison test, where $^{*}P < 0.05$, $^{**}P < 0.01$, and $^{***}P < 0.001$.

induced stress but were not toxic over 16 h (Fig. 1A). After 16 h, 25 μM 27OH-C caused a significant loss of viability, which could be prevented by co-incubation with a thiol donor, NAC (Fig. 1B). Using nontoxic concentrations of 27OH-C at 16 h (10 μM), we observed a dose-dependent decline of the GSH/GSSG ratio up to 50% without effect on viability (Fig. 1C). This was largely due to loss of GSH while GSSG remained unchanged, and the decrease in GSH/GSSG was inhibited by 3 mM NAC (data not shown). Consistent with previously reported findings, we also observed an increase in Aβ secretion from SH-SY5Y cells over 16 h in the presence of a nontoxic concentration of 27OH-C and this effect was prevented by both NAC and the acid sphingomyelinase inhibitor desipramine (Fig. 1D).

OxLDL induces a decrease in SH-SY5Y cell viability that is lipid-dependent

To simulate minimally modified LDL found in the plasma of patients with hypercholesterolemia and dementia, native LDL was incubated with 10 μM $CuSO_4$ for 1 h. This increased the

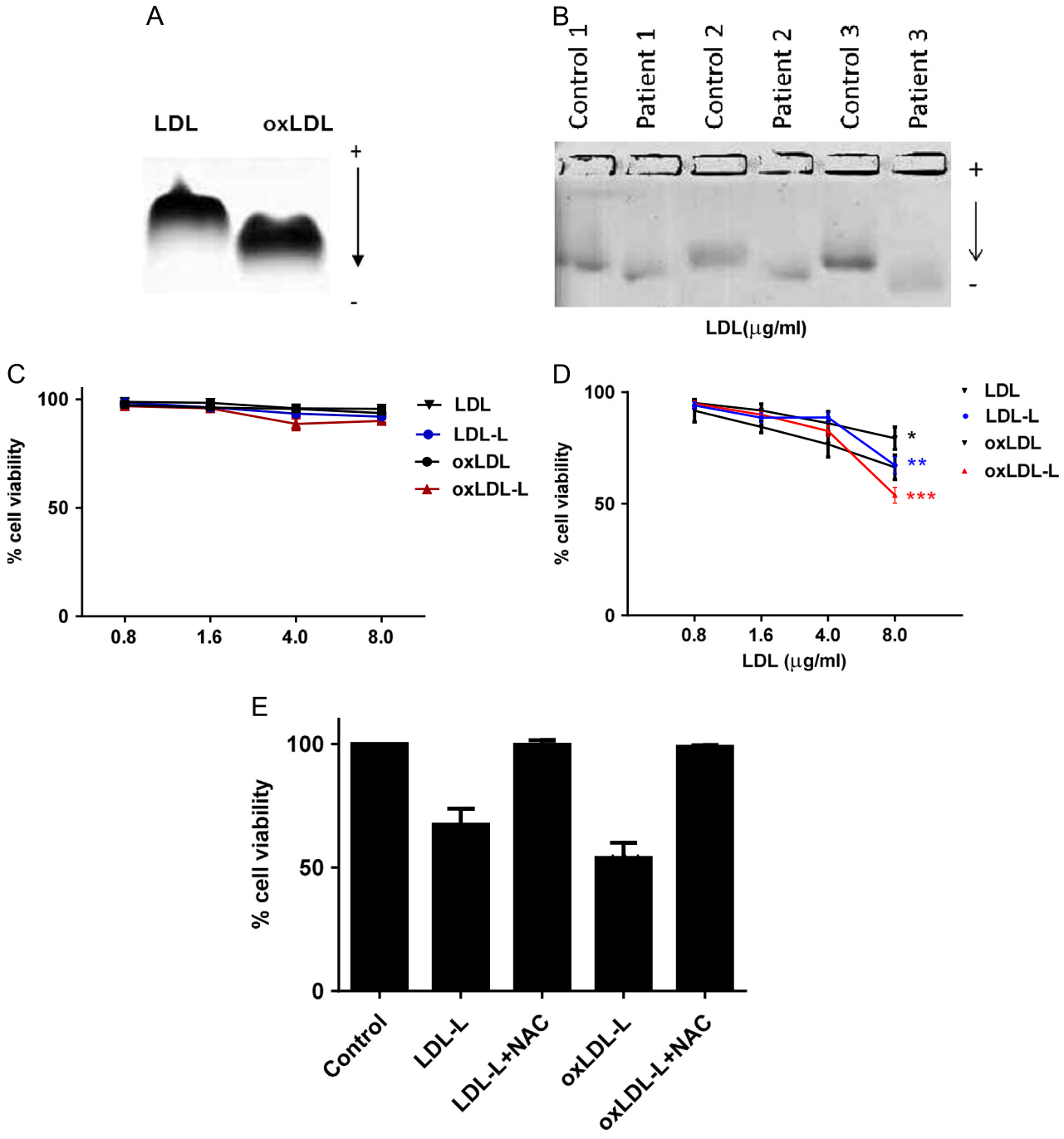

Fig. 2. SH-SY5Y viability after lipid treatments. (A) Plasma LDL (200 μg/ml) was incubated at 37 °C for 1 h in the presence of $CuSO_4$ (10 μM). (B) LDL was isolated from age- and sex-matched AD patients and control plasma ($n = 3$). Electrophoretic mobility of LDL was measured on an agarose gel. (C and D) SH-SY5Y cells were challenged with 0.8–8 μg of LDL, oxLDL, or their extracted lipids (-L) for (C) 2 or (D) 16 h. Data variance was less than 5%. (E) SH-SY5Y cells were treated with 8 μg of LDL-L or oxLDL-L in the presence of 3 mM NAC (mean ± SEM). Cell viability was measured by the MTT assay. Results are from three independent experiments. Significant differences were calculated using one-way ANOVA followed by Tukey's multiple comparison test, where $^{*}P < 0.05$, $^{**}P < 0.01$, and $^{***}P < 0.001$.

electrophoretic mobility on agarose gel (R_f: 0.49 ± 0.04) compared to untreated LDL (R_f: 0.38 ± 0.05; Fig. 2A), suggesting the loss of positive charge on basic amino acids, e.g., lysine residues, due to conjugation with MDA. This observation was consistent with the electrophoretic mobility on agarose gel (R_f: 0.51 ± 0.12; Fig. 2B) of LDL isolated from Alzheimer disease patients (Table 1) compared to age- and sex-matched healthy controls (R_f: 0.4 ± 0.11). The degree of lipid oxidation of LDL and oxLDL was determined as 8-isoprostane F2α levels (15.5 ± 1 pg/mg of LDL and 26 ± 2.5 pg/mg of oxLDL). The occurrence of phospholipid oxidation in oxLDL was supported by MS/MS analysis, which showed the presence of chain-shortened oxidized products (Supplementary Fig. 1) in agreement with the literature [30]. Cell viability was not affected by any LDL, oxLDL, or lipid treatment within 2 h (Fig. 2C). At 16 h, the viability of LDL-treated SH-SY5Y cells was not significantly decreased at any concentration tested (Fig. 2D) and oxLDL-extracted protein did not have any effect on viability either (data not shown). In contrast, 8 μg oxLDL decreased the cell viability significantly by 34% ($P < 0.05$) and lipids extracted from oxLDL resulted in 45% cell loss (Fig. 2D; $P < 0.01$); toxicity could be prevented by co-incubation with 3 mM NAC (Fig. 2E).

Table 1
Demographics of patient populations.

	Controls ($n = 10$)	AD ($n = 10$)
Age (years)	71 ± 0.3	81.6 ± 1.4
BMI (kg/m^2)	23.7 ± 0.34	24.1 ± 0.69
Total cholesterol (mmol/L)	5.67 ± 0.17	5.24 ± 0.32
LDL cholesterol (mg/dl)	121.5 ± 7.6	113.2 ± 11.1

LDL, oxLDL, and their lipids deplete intracellular GSH level and GSH/GSSG ratio in SH-SY5Y cells

We investigated whether intracellular GSH concentration was affected by nontoxic concentrations of LDL and oxLDL and their lipids; Fig. 3A confirms that despite the lack of toxicity, after 2 h treatment with 4 μg/ml LDL, GSH was significantly decreased ($P < 0.05$). Furthermore, lower concentrations (1.6 and 4 μg/ml) of

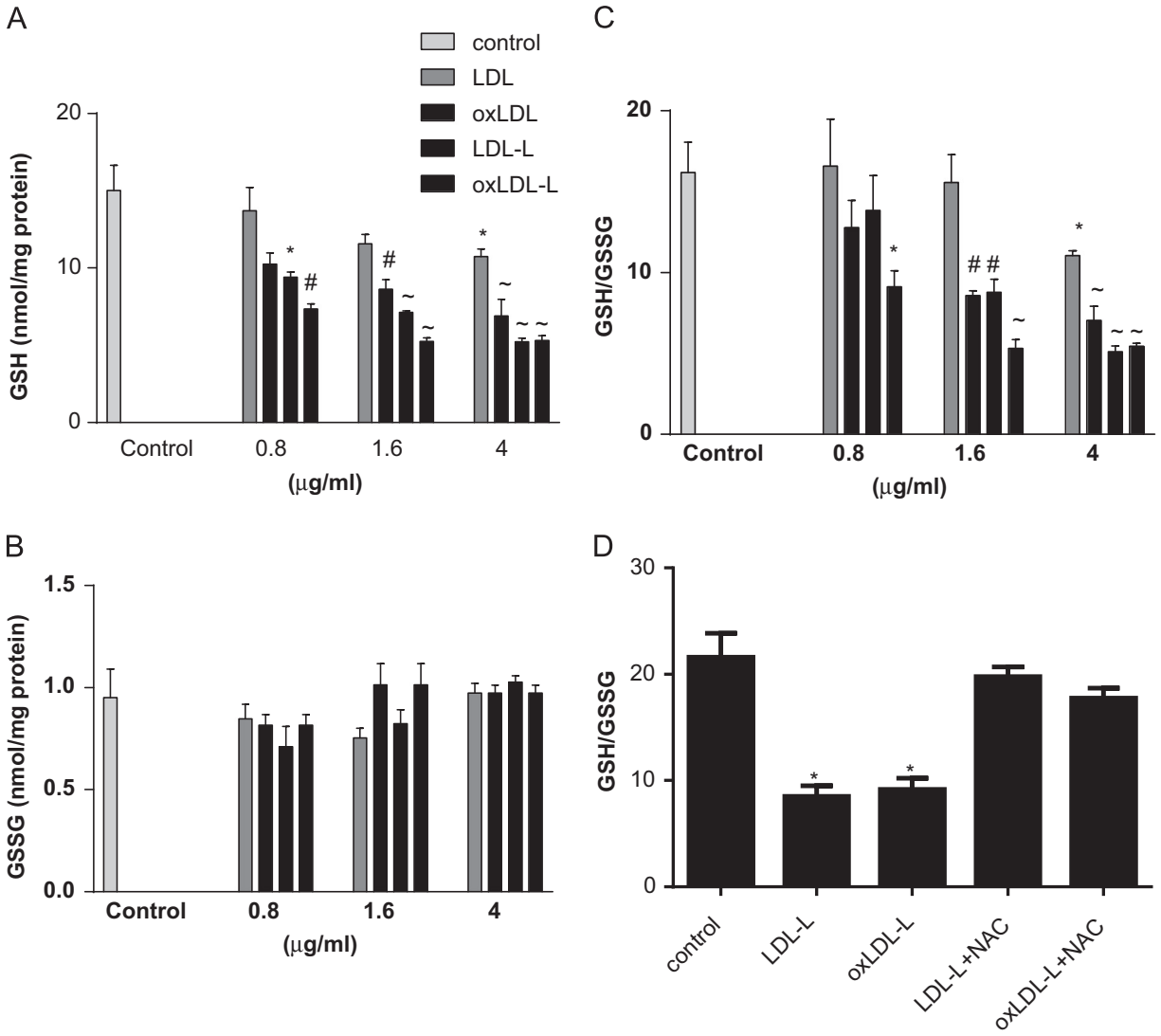

Fig. 3. LDL, oxLDL, and their extracted lipids decrease the GSH/GSSG ratio in SH-SY5Y cells. SH-SY5Y cells were treated with 0.8, 1.6, or 4 μg of LDL, oxLDL, or their lipids (-L) for 2 h. Intracellular (A) GSH and (B) GSSG levels were measured by GSH recycling assay and the GSH/GSSG ratio is shown in (C). Protein levels were measured by BCA assay. (D) Intracellular GSH and GSSG levels were measured after treating cells with LDL-L or oxLDL-L for 2 h in the presence or absence of a thiol donor, 3 mM NAC. Results are from three independent experiments and show the mean ± SEM. Significant differences were calculated using one-way ANOVA followed by Tukey's multiple comparison test, where $^{*}P < 0.05$, $^{\#}P < 0.01$, and $^{\sim}P < 0.001$.

oxLDL decreased intracellular GSH concentration to a greater extent ($P < 0.01$ and $P < 0.001$, respectively).

Lipids isolated from LDL effectively depleted intracellular GSH levels at much lower concentrations than for intact LDL: 0.8 μg/ml LDL-L, 9.4 ± 0.59 nmol GSH/mg of protein, $P < 0.05$; 1.6 μg/ml LDL-L, 7.13 ± 0.11 nmol GSH/mg of protein, $P < 0.001$; and 4 μg/ml LDL-L, 5.22 ± 0.26 nmol GSH/mg of protein, $P < 0.001$. Greater GSH depletion was observed with lipids isolated from oxLDL compared to those isolated from native LDL (Fig. 3A). Intracellular GSSG concentrations were not different between control and treatments (Fig. 3B). Nevertheless, the ratio of reduced to oxidized GSH was significantly decreased (Fig. 3C) after LDL, oxLDL, and lipid treatments. Co-incubation with NAC was sufficient to prevent the alteration in reduced to oxidized GSH observed in SH-SY5Y cells after treatment with LDL and oxLDL lipids (Fig. 3D).

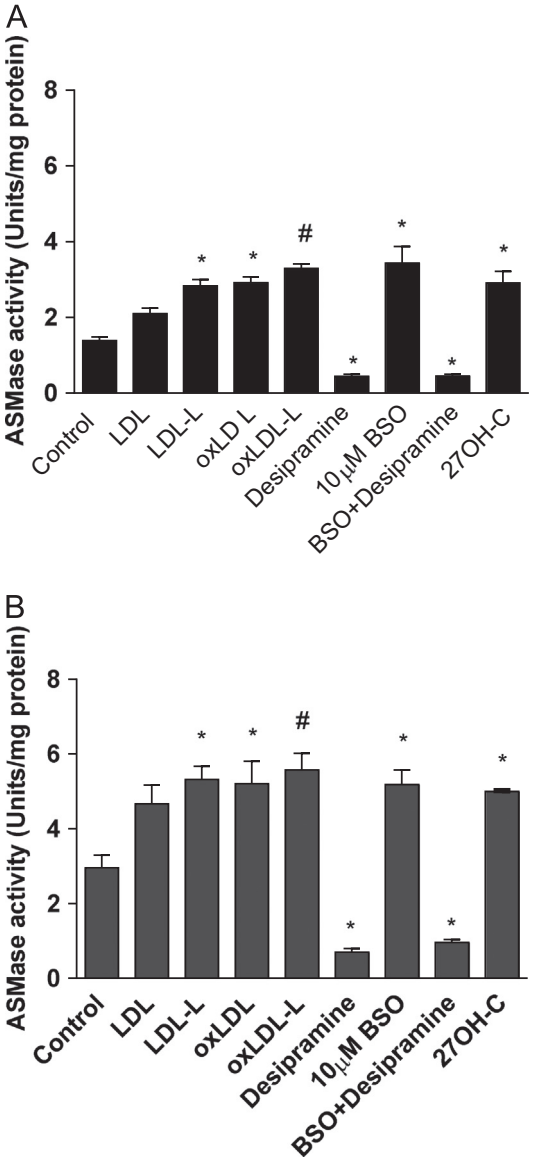

Fig. 4. Effects of 27OH-C, LDL, oxLDL, and their lipids on ASMase activity. SH-SY5Y cells were pretreated with LDL, oxLDL, or their lipids (4 μg of protein) for (A) 2 or (B) 16 h. Pretreated or untreated cells were further incubated with 10 μM desipramine, an inhibitor of acid sphingomyelinase, for 1 h before ASMase activity was measured. Results are from three independent experiments ($n = 3$). Significant differences were calculated using one-way ANOVA followed by Tukey's multiple comparison test, where $^{*}P < 0.05$ and $^{\#}P < 0.01$.

27OH-C, LDL, oxLDL, and their lipids increase acid sphingomyelinase activity

To explore whether 27OH-C or LDL could modulate ASMase activity, SH-SY5Y cells were treated with 27OH-C, LDL, oxLDL, or lipids extracted from LDL and oxLDL. After 2 h of treatment (Fig. 4A) ASMase activity was significantly increased under all the conditions tested (2.9 ± 0.31, 2.1 ± 0.14, 2.9 ± 0.15, 2.8 ± 0.16, 3.3 ± 0.11 U/mg protein) compared to untreated cells (1.4 ± 0.1 U/mg protein). After 16 h treatment (Fig. 4B), ASMase activity was increased significantly (5.0 ± 0.02, 5.32 ± 0.35 U/mg protein, $P < 0.05$; 5.21 ± 0.6 U/mg protein, $P < 0.05$; and 5.58 ± 0.44 U/mg protein, $P < 0.01$, respectively) compared to the control cells (2.96 ± 0.34 U/mg protein).

Further confirmation that GSH depletion was involved in the activation of ASMase was established by using buthionine sulfoximine (BSO). BSO, an inhibitor of γ-glutamylcysteinyl ligase, the rate-limiting enzyme for GSH synthesis and an effective agent for depleting intracellular GSH, caused an increase in ASMase activity. Desipramine (10 μM) significantly decreased the ASMase activity in both control (0.69 ± 0.1 U/mg protein) and BSO-treated cells (0.96 ± 0.07 U/mg protein; $P < 0.05$).

OxLDL lipids increase lipid raft formation

To determine the effect of intracellular redox status on the redistribution of membrane lipids, lipid rafts were labeled with cholera toxin subunit B, which also detects glycosylphosphatidylinositol (GPI)-anchored proteins and GM1 ganglioside [29] (Fig. 5A–H). Raft formation was promoted by oxidized lipids after 2 h but there was no significant raft presence at 16 h (data not shown).

SH-SYSY cell membranes were analyzed for detergent-insoluble regions by sucrose density gradient ultracentrifugation and stained for the raft marker flotillin. Lipids isolated from SH-SY5Y cells treated with minimally oxidized LDL, 27OH-C, and BSO increased lipid raft domains at 2 h. Desipramine inhibited lipid raft formation. Treatment of SH-SY5Y cells with LDL, oxLDL, their lipids (4 μg of LDL protein), and oxidized cholesterol (10 μM 27OH-C) promoted the redistribution of flotillin, a lipid raft marker, to the major raft fraction 3 (Fig. 5I). There was no significant raft presence after 16 h (data not shown).

BACE1 activity and β-amyloid production in SH-SY5Y is increased by LDL and GSH depletion

The regulation of BACE1 and its access to APP is lipid dependent and involves lipid rafts [8]; therefore, we explored whether BACE1 activity was increased by oxLDL and native LDL and their lipids. Fig. 6A confirms that after 2 h treatment with 27OH-C, BSO, LDL, oxLDL, or their lipids the activity of BACE1 was significantly increased (160 ± 7.2, 161.6 ± 9.0, 146.3 ± 5.5, 209.7 ± 9.4, 134.5 ± 5.7, 203.9 ± 12.04 U) compared to untreated cells (64.12 ± 8.2 U). This effect could be mimicked by depletion of GSH using BSO. However, by 16 h the increases in BACE1 activity by treatments were less than those observed at 2 h and not significantly increased by any of the treatments (Fig. 6B).

Given the early increase in BACE1 activity within SH-SY5Y cells exposed to 27OH-C, LDL, and oxLDL, we explored whether APP and Aβ levels were also modulated under these conditions. Fig. 6C confirms that Aβ release is increased by oxLDL lipids. 27OH-C mimicked the effects of oxLDL on the release of Aβ.

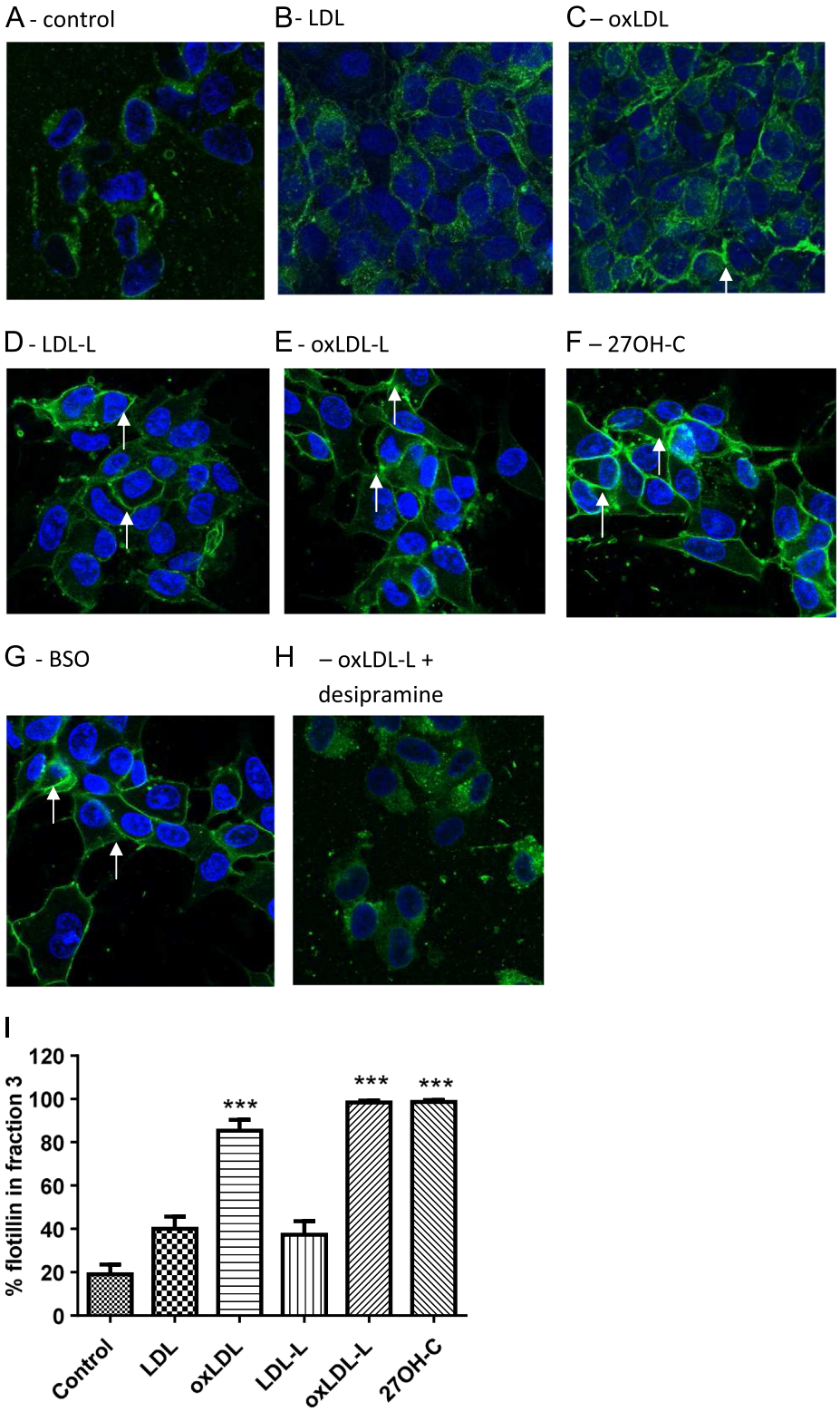

Fig. 5. 27OH-C, BSO, LDL, oxLDL, and their lipids increase the distribution of flotillin into lipid rafts of SH-SY5Y cells. SH-SY5Y cells were treated with (A) vehicle control, (B) LDL, (C) oxLDL, (D) LDL-L, (E) oxLDL-L, (F) 27OH-C, (G) BSO, and (H) desipramine with oxLDL-L for 2 h, labeled for GPI-anchored proteins with cholera toxin B (green), stained for nuclei with DAPI (blue), and analyzed by confocal microscopy. White arrows indicate strongly staining raft regions. (I) Cells treated with LDL, oxLDL, and their lipids were extracted with 1% Triton X-100 lysis buffer and applied to discontinuous sucrose gradients. Proteins were extracted and the blot was analyzed for the lipid raft marker protein flotillin-1. Flotillin-1 distribution into lipid raft fraction 3 was expressed as a % of total flotillin in all fractions. Significant differences were calculated using one-way ANOVA followed by Tukey's multiple comparison test, where $^{***}P < 0.001$. Images are representative of three independent experiments ($n = 3$).

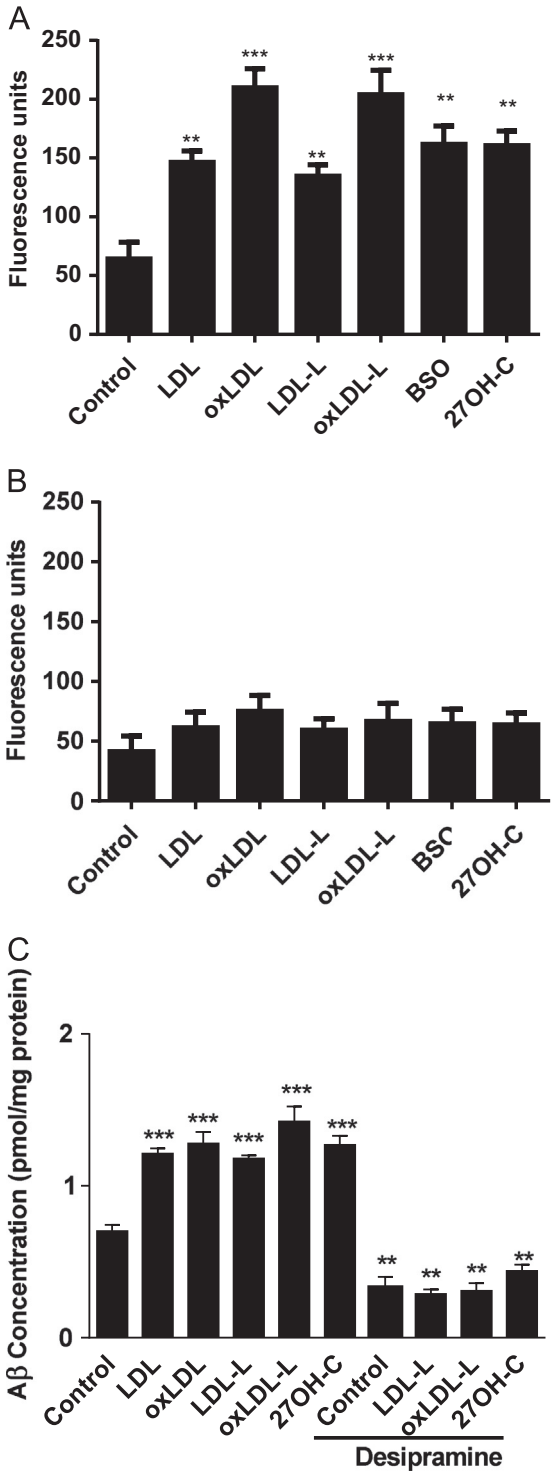

Fig. 6. 27OH-C, LDL, oxLDL, and their lipids (from 4 μg of LDL) increase BACE1 activity and β-amyloid secretion by SH-SY5Y cells. BACE1 activity was measured using a BACE1 kit (Calbiochem, Millipore) after treatment with 4 μg LDL, oxLDL, or their lipids; 10 μM BSO; or 10 μM 27OH-C at (A) 2 and (B) 16 h. (C) SH-SY5Y cells were treated with 4 μg LDL, oxLDL, or their lipids or 10 μM 27OH-C in the presence or absence of desipramine for 16 h. Supernatants were probed for β-amyloid by ELISA. Results are from three independent experiments. Significant differences were calculated using one-way ANOVA followed by Tukey's multiple comparison test, where $^{**}P < 0.01$ and $^{***}P < 0.001$.

Comparison of LDL-L and oxLDL-L lipid profiles by MS

To investigate the presence of oxidized cholesterol in lipid extracts from LDL and oxLDL, we used positive-ion electrospray mass spectrometry with scanning for precursors of *m/z* 369 to detect ions containing the cholesterol core. As shown in Fig. 7A and B, we observed a dominant cholesterol ion at *m/z* 369 corresponding to the $[M+H-H_2O]^+$ species, and the $[M+NH_4]^+$ species at *m/z* 404 also gave a strong signal. A signal at *m/z* 666 could be consistent with the presence of cholesterol linoleate. Oxidation of LDL resulted in the appearance of signals at *m/z* 544 and 558, corresponding to cholesterol esters with ω-oxidized truncated acyl chains (C8 and C9, respectively). These products have been detected previously in human vascular lesions [31]. Oxidation products of the cholesterol core do not produce the diagnostic *m/z* 369 ion upon collision-induced dissociation (CID) [31] and could not be observed using this method.

Discussion

Here, we have shown that oxidized lipid-driven membrane remodeling, which requires glutathione depletion and sphingomyelinase activation, increases β-amyloid secretion from SH-SY5Y cells through BACE1, supporting a unifying hypothesis for the involvement of systemic LDL oxidation and neurodegeneration. We have previously shown that LDL is more oxidized in the plasma of dementia patients, although total cholesterol levels remained unchanged [11]. Peripheral oxLDL is a likely source for oxidized lipid accumulation in aging brains and the transport of lipoproteins such as oxLDL into the brain is increased after the loss of BBB integrity with aging [32]. Similarly, extravascular modified LDL has been shown to cause injury through oxidative damage in the retina, which is metabolically supported through blood–retinal barrier [33]. There is strong evidence from cross-sectional and observational studies for an association between elevated serum cholesterol in midlife and later development of AD [34]. Recently, a number of comorbidities have been associated with increased risk of developing AD, including hypercholesterolemia and type 2 diabetes [12]; these conditions also associate with increased systemically oxidized lipids and may be potential modifiable risk factors for AD [1].

SH-SY5Y neuroblastoma cells are a subline of the parental line SK-N-SH and are positive for tyrosine hydroxylase and dopamine-β-hydroxylase, characteristic of catecholaminergic neurons [35]. SH-SY5Y cells express APP and secretases [36], and previous studies have shown oxysterol-mediated Aβ release in this system [23].

Lipid peroxides are detoxified intracellularly through the GSH/glutathione peroxidase/glutathione reductase cycle, resulting in a net consumption of GSH [37]. Of the LDL, oxLDL, and extracted lipids studied here, oxLDL-lipid treatments exhibit the greatest direct toxicity and early depletion of intracellular GSH in SH-SY5Y cells. However, neuronal loss in AD is a consequence of the gradual accumulation of toxic β-amyloid aggregates over decades rather a consequence of acute stress; therefore we focused on nontoxic concentrations of lipids to investigate oxLDL-lipid effects on β-amyloid production. We also investigated 27OH-C, which is a major oxysterol in oxLDL formed in the periphery, but which crosses the blood–brain barrier when the barrier is dysfunctional. This oxysterol has been reported previously to antagonize the protective effect of 24OH-C against generation of neurotoxic β-amyloid [23]. However, 24OH-C is also reported to promote the binding, uptake, and toxicity of β-amyloid to neurons [38].

After LDL, oxLDL, or 27OH-C exposure, GSH depletion occurred within 2 h in SH-SY5Y cells. GSH and its oxidized form GSSG are major contributors to cellular redox balance [39]. Cellular GSH homeostasis is dependent on the activity of glutamate–cysteine ligase (GCL) and cysteine availability [40]; expression of the rate-limiting enzyme GCL is coupled to cellular redox state through the Nrf2–Keap1 system, providing a mechanism for cellular adaptation

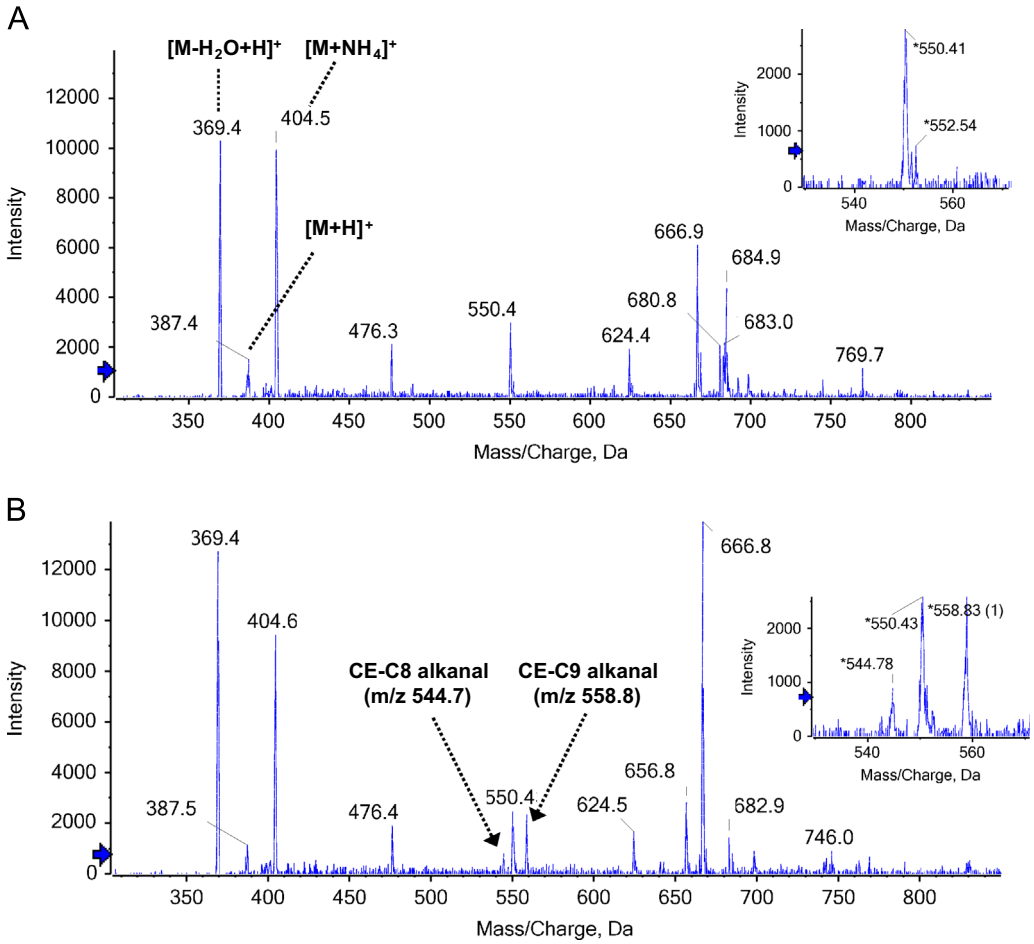

Fig. 7. ESI analysis of cholesterol and cholesteryl esters extracted from LDL and oxLDL. (A) Precursors of *m/z* 369 (*m/z* 200–900) total ion chromatogram of LDL-L. (B) Precursor ion scan of *m/z* 369.4 total ion chromatogram of oxLDL-L lipid extract. The region of the spectrum showing the appearance of signals (*m/z* 544 and 558) related to LDL oxidation is shown in the inset.

to oxidative stress through de novo GSH biosynthesis [40]. Therefore, in healthy cells the loss of GSH after removal of lipid peroxides should give rise to an increase in de novo GSH synthesis with restoration of the cellular redox state. Indeed, when using nontoxic concentrations of oxLDL, 27OH-C, and lipids, which induced GSH loss, we observed that after 16 h the GSH was restored to control levels, which is indicative of adaptation (data not shown). GSSG concentrations were not altered significantly during treatments, probably owing to the efficient export of oxidized GSSG or its involvement in mixed-disulfide formation with cellular proteins to maintain a low steady-state intracellular concentration of GSSG.

A loss of GSH without cytotoxicity, such as that observed with oxLDL, 27OH-C, or BSO treatment, can activate redox-sensitive enzymes. Acid and neutral SMase are redox-regulated enzymes [41–43] that hydrolyze sphingomyelin to ceramide and phosphocholine. Activation of ASMase correlates with translocation of the enzyme from intracellular stores to the extracellular leaflet of the cell membrane [41]. ASMase generates transient ceramide accumulation in acidic cellular compartments within minutes. There is considerable evidence that ceramides induce lipid raft clustering into unusually large raft domains in plasma membranes called “ceramide-enriched membrane platforms” [44,45]. A thiol group stabilizes the inactive conformation of ASMases forming hydrogen bonds with adjacent electron donors. Deprotonation of the thiol group and formation of an intermediate thioester bond mediates the “cysteine switch” activation mechanism [46]. Here we have confirmed that ASMase showed greatest activation within 2 h of oxLDL and lipid treatment. Moreover, using confocal microscopy and sucrose density gradient centrifugation we showed that lipid raft formation was also increased under these conditions. Even though ASMase activity was still elevated at 16 h, BACE activation or lipid raft assembly was not observed. This may be due to internalization of lipid rafts and associated protein into endosomes [47]. Activity of ASMase was inhibited by the tricyclic antidepressant drug desipramine, which also acts as a direct ligand at the α (2A) adrenergic receptor [48].

The formation of Aβ follows cleavage of APP first by BACE1, which allows further processing by γ-secretase to produce the 4-kDa Aβ peptide. Lipid raft formation has been previously reported to promote the membrane association of APP, presenilin, and BACE1 and to increase Aβ production. Here, oxLDL lipids, GSH depletion, and 27OH-C treatment increased β-amyloid secretion into the medium. OxLDL induced the largest increase in Aβ secreted from SH-SY5Y cells. Although Aβ is usually degraded after it is formed, the increase in secreted Aβ levels may be in part a result of the cell's inability to degrade Aβ, e.g., through proteasomal inhibition and failure of autophagy [49]. OxLDL is known to impair proteasome activity, offering further explanation for the failure to clear any increased concentrations of Aβ in the presence of oxidized lipids [50].

Recent findings using in vitro systems have shown upregulation of β-secretase activity and Aβ release after 27-OHC treatment [23,38,51]. Aligned with our findings, Gamba et al. [38] found that

BACE activity was prevented when cells were pretreated with NAC. This suggests the involvement of the redox environment in 27-OHC-induced Aβ secretion [38]. A rare hereditary disease, spastic paresis, is characterized by massive neurodegeneration associated with high levels of 27OH-C, one of the major oxidized lipids found in LDL, in plasma and cerebrospinal fluid (CSF) [14]. Shafatti et al. [13] demonstrated a modest accumulation of 27OH-C in brains of patients with sporadic AD; a fourfold accumulation of 27OH-C (7.8 ± 1.8 ng 27OH-C/mg tissue compared with 1.8 ± 0.8 ng 27OH-C/mg tissue in control tissue from cortex) was observed in different regions of the cortexes of patients carrying the Swedish amyloid precursor protein (APPswe) 670/671 mutation, further implicating oxidized lipids in the pathogenesis of AD. In addition to the previous report of an increase in BACE1 gene expression and Aβ formation after 27OH-C treatment in SH-SY5Y cells, our study shows that GSH concentration-dependent lipid raft formation is a key regulator of BACE1 activity and Aβ secretion.

The present findings support the importance of managing cholesterol levels to minimize the potential for LDL-lipid modification by oxidation, or perhaps by glycation during diabetes. Bayer-Carter and colleagues [52] showed that a high-saturated-fat, high-sugar diet for a month, compared to a diet low in saturated fats and simple sugars, caused significant and opposing changes in several CSF biomarkers, including dramatic changes in Aβ42 in elderly subjects. According to the population attributable risks estimates of Barnes and Yaffe, 2% of dementia cases worldwide are due to diabetes, so that a 10% lower prevalence of diabetes would lead to about 81,000 fewer cases of AD [53].

In summary, this study showed that nontoxic concentrations of oxLDL lipids and 27OH-C decrease GSH/GSSG ratio and increase extracellular Aβ secretion by SH-SY5Y cells through activation of sphingomyelinase. This work offers an explanation for the association between hypercholesterolemia, increased plasma levels of oxLDL, Aβ accumulation, neuronal loss, and the onset of AD. Reducing LDL oxidation in midlife could provide an important therapeutic strategy for delaying AD onset and progression. Importantly this work also suggests that sphingomyelinase offers a novel target to mitigate the effects of oxLDL lipid stress.

Acknowledgments

The authors acknowledge financial support from The Dunhill Medical Trust (Grant R92/1108). H.R.G. and C.M.S. also acknowledge support through the COST CM1001 and COST BM1023 programs. A.R. acknowledges funding for a Marie-Curie Intra-European Fellowship (FP7-PEOPLE-2009-IEF Project ID 255076 “ATHERO_MASS”). The confocal scanning multiphoton microscope was provided by Aston Research Centre for Healthy Ageing.

Appendix A. Supplementary material

Supplementary data associated with this article can be found in the online version at http://dx.doi.org/10.1016/j.freeradbiomed.2014.07.012.

References

[1] Ballard, C.; Gauthier, S.; Corbett, A.; Brayne, C.; Aarsland, D.; Jones, E. Alzheimer's disease. *Lancet* **377:**1019–1031; 2011.
[2] Hussain, I.; Powell, D.; Howlett, D. R.; Tew, D. G.; Meek, T. D.; Chapman, C.; Gloger, I. S.; Murphy, K. E.; Southan, C. D.; Ryan, D. M.; Smith, T. S.; Simmons, D. L.; Walsh, F. S.; Dingwall, C.; Christie, G. Identification of a novel aspartic protease (Asp 2) as beta-secretase. *Mol. Cell. Neurosci.* **14:**419–427; 1999.
[3] Lambert, J.; Heath, S.; Even, G.; Campion, D.; Sleegers, K.; Hiltunen, M.; Combarros, O.; Zelenika, D.; Bullido, M.; Tavernier, B.; et al. Genome-wide association study identifies variants at CLU and CR1 associated with Alzheimer's disease. *Nat. Genet.* **41:**1094–1099; 2009.
[4] Hollingworth, P.; Harold, D.; Sims, R.; Gerrish, A.; Lambert, J. C.; Carrasquillo, M. M.; Abraham, R.; Hamshere, M. L.; Pahwa, J. S.; Moskvina, V.; et al. Common variants at ABCA7, MS4A6A/MS4A4E, EPHA1, CD33 and CD2AP are associated with Alzheimer's disease. *Nat. Genet.* **43:**429–435; 2011.
[5] Naj, A. C.; Jun, G.; Beecham, G. W.; Wang, L. S.; Vardarajan, B. N.; Buros, J.; Gallins, P. J.; Buxbaum, J. D.; Jarvik, G. P.; Crane, P. K.; et al. Common variants at MS4A4/MS4A6E, CD2AP, CD33 and EPHA1 are associated with late-onset Alzheimer's disease. *Nat. Genet.* **43:**436–441; 2011.
[6] Chan, R. B.; Oliveira, T. G.; Cortes, E. P.; Honig, L. S.; Duff, K. E.; Small, S. A.; Wenk, M. R.; Shui, G.; Di Paolo, G. Comparative lipidomic analysis of mouse and human brain with Alzheimer disease. *J. Biol. Chem.* **287:**2678–2688; 2012.
[7] Mapstone, M.; Cheema, A. K.; Fiandaca, M. S. Plasma phospholipids identify antecedent memory impairment in older adults. *Nat. Med.* **20:**415–418; 2014.
[8] Kalvodova, L.; Kahya, N.; Schwille, P.; Ehehalt, R.; Verkade, P.; Drechsel, D.; Simons, K. Lipids as modulators of proteolytic activity of BACE: involvement of cholesterol, glycosphingolipids, and anionic phospholipids in vitro. *J. Biol. Chem.* **280:**36815–36823; 2005.
[9] Grimm, M. O.; Grimm, H. S.; Patzold, A. J.; Zinser, E. G.; Halonen, R.; Duering, M.; Tschape, J. A.; De Strooper, B.; Muller, U.; Shen, J.; Hartmann, T. Regulation of cholesterol and sphingomyelin metabolism by amyloid-beta and presenilin. *Nat. Cell Biol.* **7:**1118–1123; 2005.
[10] Matsuzaki, K.; Kato, K.; Yanagisawa, K. Abeta polymerization through interaction with membrane gangliosides. *Biochim. Biophys. Acta* **1801:**868–877; 2010.
[11] Li, L.; Willets, R. S.; Polidori, M. C.; Stahl, W.; Nelles, G.; Sies, H.; Griffiths, H. R. Oxidative LDL modification is increased in vascular dementia and is inversely associated with cognitive performance. *Free Radic. Res.* **44:**241–248; 2010.
[12] Polidori, M. C.; Pientka, L.; Nelles, G.; Griffiths, H. R. Modulation of cholesterol in midlife affords cognitive advantage during ageing—a role for altered redox balance. *Int. J. Clin. Exp. Med.* **3:**103–109; 2010.
[13] Shafaati, M.; Marutle, A.; Pettersson, H.; Lövgren-Sandblom, A.; Olin, M.; Pikuleva, I.; Winblad, B.; Nordberg, A.; Björkhem, I. Marked accumulation of 27-hydroxycholesterol in the brains of Alzheimer's patients with the Swedish APP 670/671 mutation. *J. Lipid Res.* **52:**1004–1010; 2011.
[14] Schüle, R.; Siddique, T.; Deng, H. -X.; Yang, Y.; Donkervoort, S.; Hansson, M.; Madrid, R. E.; Siddique, N.; Schöls, L.; Björkhem, I. Marked accumulation of 27-hydroxycholesterol in SPG5 patients with hereditary spastic paresis. *J. Lipid Res.* **51:**819–823; 2010.
[15] Shafaati, M.; Marutle, A.; Pettersson, H.; Lovgren-Sandblom, A.; Olin, M.; Pikuleva, I.; Winblad, B.; Nordberg, A.; Bjorkhem, I. Marked accumulation of 27-hydroxycholesterol in the brains of Alzheimer's patients with the Swedish APP 670/671 mutation. *J. Lipid Res.* **52:**1004–1010; 2011.
[16] Slooter, A. J.; Cruts, M.; Kalmijn, S.; Hofman, A.; Breteler, M. M.; Van Broeckhoven, C.; van Duijn, C. M. Risk estimates of dementia by apolipoprotein E genotypes from a population-based incidence study: the Rotterdam Study. *Arch. Neurol.* **55:**964–968; 1998.
[17] Reis, A.; Rudnitskaya, A.; Blackburn, G. J.; Fauzi, N. M.; Pitt, A. R.; Spickett, C. M. A comparison of five lipid extraction solvent systems for lipidomic studies of human LDL. *J. Lipid Res.* **54:**1812–1824; 2013.
[18] Lewis, T. L.; Cao, D.; Lu, H.; Mans, R. A.; Su, Y. R.; Jungbauer, L.; Linton, M. F.; Fazio, S.; LaDu, M. J.; Li, L. Overexpression of human apolipoprotein A-I preserves cognitive function and attenuates neuroinflammation and cerebral amyloid angiopathy in a mouse model of Alzheimer disease. *J. Biol. Chem.* **285:**36958–36968; 2010.
[19] Dias, I. H.; Polidori, M. C.; Li, L.; Weber, D.; Stahl, W.; Nelles, G.; Grune, T.; Griffiths, H. R. Plasma levels of HDL and carotenoids are lower in dementia patients with vascular comorbidities. *J. Alzheimers Dis.* **40:**399–408; 2013.
[20] Baird, S. K.; Reid, L.; Hampton, M. B.; Gieseg, S. P. OxLDL induced cell death is inhibited by the macrophage synthesised pterin, 7,8-dihydroneopterin, in U937 cells but not THP-1 cells. *Biochim. Biophys. Acta* **1745:**361–369; 2005.
[21] Soeda, S.; Tsuji, Y.; Ochiai, T.; Mishima, K.; Iwasaki, K.; Fujiwara, M.; Yokomatsu, T.; Murano, T.; Shibuya, S.; Shimeno, H. Inhibition of sphingomyelinase activity helps to prevent neuron death caused by ischemic stress. *Neurochem. Int.* **45:**619–626; 2004.
[22] Marwarha, G.; Dasari, B.; Prasanthi, J. R.; Schommer, J.; Ghribi, O. Leptin reduces the accumulation of Abeta and phosphorylated tau induced by 27-hydroxycholesterol in rabbit organotypic slices. *J. Alzheimers Dis.* **19:**1007–1019; 2010.
[23] Prasanthi, J. R.; Huls, A.; Thomasson, S.; Thompson, A.; Schommer, E.; Ghribi, O. Differential effects of 24-hydroxycholesterol and 27-hydroxycholesterol on beta-amyloid precursor protein levels and processing in human neuroblastoma SH-SY5Y cells. *Mol. Neurodegener.* **4:**1; 2009.
[24] Marwarha, G.; Raza, S.; Prasanthi, J. R. P.; Ghribi, O. Gadd153 and NF-κB crosstalk regulates 27-hydroxycholesterol-induced increase in BACE1 and β-amyloid production in human neuroblastoma SH-SY5Y cells. *PLoS One* **8:** e70773; 2013.
[25] Gao, D.; Pararasa, C.; Dunston, C. R.; Bailey, C. J.; Griffiths, H. R. Palmitate promotes monocyte atherogenicity via de novo ceramide synthesis. *Free Radic. Biol. Med.* **53:**796–806; 2012.
[26] Griffiths, H. R.; Aldred, S.; Dale, C.; Nakano, E.; Kitas, G. D.; Grant, M. G.; Nugent, D.; Taiwo, F. A.; Li, L.; Powers, H. J. Homocysteine from endothelial cells promotes LDL nitration and scavenger receptor uptake. *Free Radic. Biol. Med.* **40:**488–500; 2006.
[27] Qin, L.; Bartlett, H.; Griffiths, H. R.; Eperjesi, F.; Armstrong, R. A.; Gherghel, D. Macular pigment optical density is related to blood glutathione levels in healthy individuals. *Invest. Ophthalmol. Visual Sci.* **52:**5029–5033; 2011.

[28] Dias, I. H.; Chapple, I. L.; Milward, M.; Grant, M. M.; Hill, E.; Brown, J.; Griffiths, H. R. Sulforaphane restores cellular glutathione levels and reduces chronic periodontitis neutrophil hyperactivity in vitro. *PLoS One* **8:**e66407; 2013.
[29] Blank, N.; Schiller, M.; Krienke, S.; Wabnitz, G.; Ho, A. D.; Lorenz, H. M. Cholera toxin binds to lipid rafts but has a limited specificity for ganglioside GM1. *Immunol. Cell Biol.* **85:**378–382; 2007.
[30] Gruber, F.; Bicker, W.; Oskolkova, O. V.; Tschachler, E.; B, V. N. A simplified procedure for semi-targeted lipidomic analysis of oxidized phosphatidylcholines induced by UVA irradiation. *J. Lipid Res.* **53:**1232–1242; 2012.
[31] Hutchins, P. M.; Moore, E. E.; M, R. C. Electrospray MS/MS reveals extensive and nonspecific oxidation of cholesterol esters in human peripheral vascular lesions. *J. Lipid Res.* **52:**2070–2083; 2011.
[32] Leoni, V.; Caccia, C. Oxysterols as biomarkers in neurodegenerative diseases. *Chem. Phys. Lipids* **164:**515–524; 2011.
[33] Du, M.; Wu, M.; Fu, D.; Yang, S.; Chen, J.; Wilson, K.; Lyons, T. J. Effects of modified LDL and HDL on retinal pigment epithelial cells: a role in diabetic retinopathy? *Diabetologia* **56:**2318–2328; 2013.
[34] Shepardson, N. E.; Shankar, G. M.; Selkoe, D. J. Cholesterol level and statin use in Alzheimer disease. I. Review of epidemiological and preclinical studies. *Arch Neurol.* **68:**1239–1244; 2011.
[35] Komada, Y.; Azuma, E.; Kamiya, H.; Sakurai, M. Phenotypic profile of human neuroblastoma cell lines: association with morphological characteristics. *Br. J. Cancer* **54:**711–715; 1986.
[36] Liu, W. W.; Todd, S.; Coulson, D. T. R.; Irvine, G. B.; Passmore, A. P.; McGuinness, B.; McConville, M.; Johnston, D. C. A novel reciprocal and biphasic relationship between membrane cholesterol and β-secretase activity in SH-SY5Y cells and in human platelets. *J. Neurochem.* **108:**341–349; 2008.
[37] Parasassi, T.; Brunelli, R.; Costa, G.; De Spirito, M.; Krasnowska, E.; Lundeberg, T.; Pittaluga, E.; F, U. Thiol redox transitions in cell signaling: a lesson from N-acetylcysteine. *ScientificWorldJournal* **10:**1192–1202; 2010.
[38] Gamba, P.; Leonarduzzi, G.; Tamagno, E.; Guglielmotto, M.; Testa, G.; Sottero, B.; Gargiulo, S.; Biasi, F.; Mauro, A.; Vina, J.; Poli, G. Interaction between 24-hydroxycholesterol, oxidative stress, and amyloid-beta in amplifying neuronal damage in Alzheimer's disease: three partners in crime. *Aging Cell* **10:**403–417; 2011.
[39] Aon, M. A.; Cortassa, S.; O'Rourke, B. Redox-optimized ROS balance: a unifying hypothesis. *Biochim. Biophys. Acta Bioenerg* **1797:**865–877; 2010.
[40] Wild, A. C.; Moinova, H. R.; Mulcahy, R. T. Regulation of γ-glutamylcysteine synthetase subunit gene expression by the transcription factor Nrf2. *J. Biol. Chem.* **274:**33627–33636; 1999.
[41] Schissel, S. L.; Keesler, G. A.; Schuchman, E. H.; Williams, K. J.; Tabas, I. The cellular trafficking and zinc dependence of secretory and lysosomal sphingomyelinase, two products of the acid sphingomyelinase gene. *J. Biol. Chem.* **273:**18250–18259; 1998.
[42] Holopainen, J. M.; Subramanian, M.; Kinnunen, P. K. J. Sphingomyelinase induces lipid microdomain formation in a fluid phosphatidylcholine/sphingomyelin membrane. *Biochemistry* **37:**17562–17570; 1998.
[43] Martin, S. F.; Sawai, H.; Villalba, J. M.; Hannun, Y. A. Redox regulation of neutral sphingomyelinase-1 activity in HEK293 cells through a GSH-dependent mechanism. *Arch. Biochem. Biophys.* **459:**295–300; 2007.
[44] Grassme, H.; Jendrossek, V.; Riehle, A.; Kurthy, G. v.; Berger, J.; Schwarz, H.; Weller, M.; Kolesnick, R.; Gulbins, E. Host defense against Pseudomonas aeruginosa requires ceramide-rich membrane rafts. *Nat. Med.* **9:**322–330; 2003.
[45] Li, P.; Zhang, Y.; Yi, F. Lipid raft redox signaling platforms in endothelial dysfunction. *Antioxid. Redox Signaling* **9:**1457–1470; 2007.
[46] Qiu, H.; Edmunds, T.; Baker-Malcolm, J.; Karey, K. P.; Estes, S.; Schwarz, C.; Hughes, H.; Van Patten, S. M. Activation of human acid sphingomyelinase through modification or deletion of C-terminal cysteine. *J. Biol. Chem.* **278:**32744–32752; 2003.
[47] Ewers, H.; Helenius, A. Lipid-mediated endocytosis. *Cold Spring Harbor Perspect. Biol.* **3:**a004721; 2011.
[48] Walton, K. A.; Gugiu, B. G.; Thomas, M.; Basseri, R. J.; Eliav, D. R.; Salomon, R. G.; B, J. A. A role for neutral sphingomyelinase activation in the inhibition of LPS action by phospholipid oxidation products. *J. Lipid Res.* **47:**1967–1974; 2006.
[49] Agholme, L.; Hallbeck, M.; Benedikz, E.; Marcusson, J.; Kagedal, K. Amyloid-beta secretion, generation, and lysosomal sequestration in response to proteasome inhibition: involvement of autophagy. *J. Alzheimers Dis.* **31:**343–358; 2012.
[50] Aytan, N.; Jung, T.; Tamturk, F.; Grune, T.; Kartal-Ozer, N. Oxidative stress related changes in the brain of hypercholesterolemic rabbits. *BioFactors (Oxford, England)* **33:**225–236; 2008.
[51] Gamba, P.; Guglielmotto, M.; Testa, G.; Monteleone, D.; Zerbinati, C.; Gargiulo, S.; Biasi, F.; Iuliano, L.; Giaccone, G.; Mauro, A.; Poli, G.; Tamagno, E.; Leonarduzzi, G. Up-regulation of β-amyloidogenesis in neuron-like human cells by both 24- and 27-hydroxycholesterol: protective effect of N-acetylcysteine. *Aging Cell* **13:**561–572; 2014.
[52] Bayer-Carter, J. L.; Green, P. S.; Montine, T. J.; VanFossen, B.; Baker, L. D.; Watson, G. S.; Bonner, L. M.; Callaghan, M.; Leverenz, J. B.; Walter, B. K.; Tsai, E.; Plymate, S. R.; Postupna, N.; Wilkinson, C. W.; Zhang, J.; Lampe, J.; Kahn, S. E.; Craft, S. Diet intervention and cerebrospinal fluid biomarkers in amnestic mild cognitive impairment. *Arch. Neurol.* **68:**743–752; 2011.
[53] Barnes, D. E.; Yaffe, K. The projected effect of risk factor reduction on Alzheimer's disease prevalence. *Lancet Neurol.* **10:**819–828; 2011.